NMR Analysis of the interaction of Ethanol with the Nicotinic Acetylcholine Receptor. [†]

David Naugler[a]*, Robert J. Cushley[a], Ian Clark-Lewis[b]**

[a]*Department of Molecular Biology and Biochemistry, Simon Fraser University, Burnaby, British Columbia, Canada V5A 1S6*

[b]*Biochemistry and Molecular Biology, University of British Columbia*

2350 Health Sciences Mall, Vancouver, BC Canada V6T 1Z3

Keywords: NMR, T_1, T_{1p}, nAChR, ethanol, K_d

* David.Naugler@utoronto.ca, ** Deceased.

Abbreviations:

C_{50}, concentration which elicits 50% of effective response; EDTA, ethylenediaminetetraacetic acid; HEPES, 4-(2-hydroxyethyl)-1-piperazineethanesulfonic acid; K_d, dissociation constant, concentration at which complex is 50% dissociated;

nAChR, nicotinic acetylcholine receptor; NMR, nuclear magnetic resonance; NOESY, nuclear Overhauser effect spectroscopy; Pi, inorganic phosphate, PO_4^{2-}; NLS, nonlinear least squares.

Abstract

Ethanol exerts its actions in the central and peripheral nervous systems through the direct interactions with several proteins, including ligand-gated ion channels such as the nicotinic acetylcholine receptor (nAChR). The binding interaction between ethanol and sodium cholate solubilized nicotinic acetylcholine receptor protein can be detected through either NMR line broadening or T_1 titration. In this paper, we examine the use of weighted Navon T_{1p} analysis of T_1 titration data for the estimation of the dissociation constant of ethanol for the nAChR. We show that Navon T_{1p} analysis underestimates binding affinity. The application of rigorous limits for confidence intervals within a nonlinear regression analysis of this data provides a best estimate of K_d = 55 μM at 4 °C. within an unsymmetrical 90% confidence interval of [0.5, 440 μM]. Accordingly, the best estimate of the binding free energy is ΔG^0 = −5.4 Kcal/mole within a 90% confidence interval of [−8.0, -4.3 Kcal/mole], relative to conventional standard states.

1. Introduction

Ethanol can exert profound effects on several components of the central and peripheral nervous systems, including ligand-gated ion channels, [1]. The effects of ethanol can be either stimulatory or inhibitory. For example, ethanol acts as a functional antagonist of ionotropic glutamate receptors [2], but stabilizes the open state of the muscle-type acetylcholine receptor [3]. Extensive studies of the effects of ethanol and other general anesthetics on ligand-gated ion channels provide convincing evidence for the notion that these compounds bind to discrete sites on the channel [4, 5].

The idea that ethanol and other general anesthetics bind to discrete sites on the channel protein has been supported by several site-directed mutagenesis studies on several different ligand-gated ion channels in which specific mutations in the pore-forming domains of the protein were found to alter the sensitivity of the receptors to ethanol [6, 7]. However, these studies should infer that the compound of interest bound to a discrete site on the receptor from looking at effects on functional properties. Due to the low affinity of ethanol (μM to mM range), it is not possible to study the interaction of ethanol with its binding site on the receptor using conventional ligand-binding techniques. However, nuclear magnetic resonance techniques can be used to study the interaction of ethanol with the receptor [8-12], and thus obtain estimates for the true affinity of ethanol for its binding site.

In this study, we have used NMR relaxation methods to estimate the binding parameters for ethanol in the presence of sodium cholate solubilized nicotinic acetylcholine receptor protein. Using this approach, we find that ethanol binds to the solubilized receptor with an affinity in the 100 μM range, and compare this value with

estimates of the affinity from measurements that depend on alteration of receptor function. In a previous study [52], we used ^{1}H chemical shifts in a nonlinear regression model.

2.   Materials and methods

2.1 Receptor protein isolation and purification

Preparation of sodium cholate solubilized nicotinic acetylcholine receptor protein generally followed the procedure of ref. [13]. All steps handling the protein were carried out at 4 °C, unless otherwise stated. Receptor rich membranes from the electroplax tissue of *Torpedo californica* were prepared from frozen electroplax (Pacific Biomarine, Venice, CA) using the procedure of Sobel et al. [14] as modified by Epstein and Racker [15]. Membranes were stored frozen at –70 °C in 0.4 M sucrose, 2 mM HEPES, pH 7.5 until used. Sucrose and HEPES were removed by dialysis against cold distilled water containing ~85 μM EDTA, which was renewed regularly over several days. Receptor rich membranes were then reduced to pellet form by ultracentrifugation at 130,000 g for 30 min. Pellets were resuspended in 'Buffer I', containing 10 mM Na phosphate, pH 8.0, 100 mM NaCl, 60 mM KCl by sonication. This was followed by ultracentrifugation at 130,000 g for 30 min., to reduce receptor rich membranes to pellet form. A second smaller batch of Buffer I was prepared using D_2O rather than H_2O. Using sonication, the receptor rich membranes pellet was resuspended in Buffer I D_2O solution and the pD adjusted to 10.6 with 1 N NaOD. Alkaline-treated membranes (2.5 mg protein /ml) in Buffer I D_2O solution were solubilized by the addition of 20% Na

cholate/D_2O to a final cholate concentration of 1%. After incubation for 20-30 min. and ultracentrifugation for 30 min at 130,000 g, the supernatant (cholate extract) was collected and the pellet (membranes) discarded.

Acetylcholine receptor concentration was determined using [^{125}I] α-bungarotoxin binding [16].

2.2 NMR

All protein NMR was done on a Bruker AMX600 operating at a ^{1}H frequency of 600.13 MHz and at a temperature of 277 °K. Thermal regulation was achieved using a Bruker Eurotherm Variable Temperature unit. Longitudinal relaxation, T_1, was studied using a conventional inversion recovery pulse program. T_1 values were estimated using the nonlinear least squares T_1/T_2 routines of Bruker UXNMR or XWinNMR software. Since the T_1 of free ethanol is 5 sec. at 277 K, this necessitated a recycle time of 25 sec. with 16 scans at each delay. Sixteen variable delays were used. The following list is typical. T_1 delays (seconds): 25, 16.6, 11.1, 7.4, 4.94, 3.292, 2.194, 1.463, 0.975, 0.650, 0.433, 0.289, 0.193, 0.128, 0.085, and 0.000004. The T_1 delays used are an important determinant of the precision versus time efficiency of T_1 estimation. Ref. [17] and references cited therein, provides an analysis for optimal estimation of longitudinal relaxation and advocates the use of unequally spaced sample points in the context of nonlinear least squares parameter estimation.   Ref. [18] provides an analysis of the problem of estimating NMR relaxation rate in the context of median estimation [19]. However, it is mathematically more tractable to treat an estimation scheme that is

analytical. In ref. [18, 20, 48-50] we develop a forward modeling approach to exponential estimation for the general relaxation model

$$f(t) = Ae^{-Lt} + B \tag{1}$$

It is shown that under reasonable assumption, the four-point spectral estimator scheme

$$Ldt = \ln((f_1 - f_3)/(f_2 - f_4)) \tag{2}$$

provides optimal estimation. In this scheme, dt is the sample delay between four equally spaced points f_1, f_2, f_3, f_4. In the context of real error, this scheme is biased, although the bias can be calculated and subtracted off. However, in the context of complex NMR error, spectral estimation [18, 20] is unbiased. We show that to second order, the standard deviation, S_2, of this estimation scheme is given as,

$$S_2 = \frac{\sigma}{|A| dt} \frac{\sqrt{2}\sqrt{1+e^{2Ldt}}}{(1-e^{-2Ldt})} \tag{3}$$

where σ is the noise level.

An analytical, forward modeling approach to an estimation problem is of great value. However, no such approach exists for the estimation problem treated in this paper. The Navon method [21, 22] initially considered here, places special emphasis on the T_1 value of the free ligand. The T_1 of 'free' ethanol was determined in a sample, which was identical in D_2O Buffer I and in sodium cholate concentration, to the others

except it lacked the 1.7 μM nAChR protein. The ethanol concentration in the 'free'

sample was 55 mM.

2.3 Longitudinal relaxation

Because the transverse relaxation phenomenon is observed on a multiplet, we

chose to investigate the concentration dependence of longitudinal relaxation.   For

two-site fast exchange, nuclear magnetic longitudinal relaxation can be expressed in a

mole fraction weighted model [23] as:

$$R_{1obs} = R'_{1b} \cdot f_b + R_{1free} \cdot f_{free} \qquad (4)$$

where, R_{1obs}, R'_{1b} and R_{1free} are the relaxation rates observed and of the bound and

free species, respectively, in Hz (1/s). Variables, f_b and f_{free} are the mole fractions of

bound and free species, respectively. These latter quantities are calculated as part of a

two-site equilibrium model, which is dependent upon the dissociation constant, K_d. The

relaxation rates of free and bound species can be related to relaxation times [21, 22] by:

$$R_{1free} = 1/T_{1free} \qquad (5)$$

which is a directly measurable quantity, and

$$R'_{1b} = 1/(T_{1bound} + \tau_{bound}) \qquad (6)$$

in which $T_{1\text{bound}}$ is the relaxation time of the bound species, intrinsic to the nucleus in question, and τ_{bound} is the bound lifetime, intrinsic to the exchange process itself. In ethanol, there are two different ^{1}H nuclei detected, the methyl and methylene protons, each with its own $R_{1\text{obs}}$, R'_{1b}, $R_{1\text{free}}$ and $T_{1\text{bound}}$. The exchange or bound lifetime is related to kinetic exchange rate by $\tau_{\text{bound}} = 1/k_{-1}$.

Since we have a method for an accurate determination of $R_{1\text{free}}$, [21, 22], we can rewrite equation (4) as:

$$RR_{1obs} = \frac{R_{1obs}}{R_{1free}} = \frac{R'_{1b}}{R_{1free}} \cdot f_b + f_{free} = RR'_{1b} \cdot f_b + f_{free} \tag{7}$$

in a reduced rate formulation. This has the advantage of allowing the comparison of like, dimensionless quantities. Table 1 shows the raw data that are transformed. The exchange process can be represented as:

$$AChR + L \underset{k_{-1}}{\overset{k_1}{\rightleftharpoons}} AChR \cdot L \tag{8}$$

where AChR represents the (nicotinic) acetylcholine receptor, L represents the ligand, ethanol, and $AChR \cdot L$ represents the receptor-ligand complex. Three equations define this two-site exchange system:

$$K_d = \frac{[AChR][L]}{[AChR \cdot L]} \tag{9}$$

defines the equilibrium condition,

$$[L]_{Tot} = [L] + [AChR \cdot L] \tag{10}$$

specifies the mass balance in ligand, and

$$[AChR]_{Tot} = [AChR] + [AChR \cdot L] \tag{11}$$

specifies the mass balance in protein.

We have a system of three equations in three unknowns that can be solved, in principle. Because we do not initially know the value of K_d, we can start with the fiction that its value is zero. This is a tight binding approximation. Since the ligand is in excess, we then have

$$[AChR \cdot L] = [AChR]_{Tot} \tag{12}$$

$$[L] = [L]_{Tot} - [AChR]_{Tot} \tag{13}$$

$$f_{free} = \frac{([L]_{Tot} - [AChR]_{Tot})}{[L]_{Tot}} \tag{14}$$

and

$$f_b = \frac{[AChR]_{Tot}}{[L]_{Tot}} \tag{15}$$

for substitution into equation (7). This gives us a model that we can regress against the raw data given in Table 1,

$$RR_{1obs} = \frac{(RR'_{1b} - 1)[AChR]_{Tot}}{[L]_{Tot}} + 1 \tag{16}$$

According to Navon analysis, error in R_{Tot} translates into error in the determination of $(T_{1b} + \tau_b)$ but not in K_d. The $(T_{1b} + \tau_b)$ values found here are like those of Navon [21]. Therefore, any errors or uncertainties in the value of $[AChR]_{TOT}$ will have little or no effect on the results.

Figure 1 shows the line broadening of ethanol that occurs in the presence of nAChR protein. The multiplet structure of ethanol is completely washed out due to a line broadening of 20 Hz. The $^3J_{HH}$ coupling constant of 7 Hz gives rise to a triplet at the methyl and a quartet at the methylene, when this can be resolved. The line broadening declines as the cholate detergent denatures the protein. Storage at 4 °C will not prevent complete denaturation over a period of a month. After denaturation, the multiplet structure of ethanol then is again seen (data not shown).

The large value for the correlation of determination for the tight binding model means that the estimation of K_d is a difficult task. The Navon method [22, 24] provides one approach. This method is an approximate linearization that is analogous to some methods of linearization of hyperbolic data in Michaelis-Menton kinetics. It relies on plotting T_{1p}, defined by,

$$T_{1p} = (1/ T_{1obs} - 1/ T_{1free})^{-1} \tag{17}$$

versus ligand concentration. Historically, the notation above was used because of the practicalities of experimental physics. An equivalent notation would have,

$$R_{1obs}([L]) = R_{1b}([L]) + R_{1free} \tag{18}$$

Conceptually, this is very compelling because with effort, it is possible to obtain a very good estimate for T_{1free}. In this approximation, K_d is determined as the negative x-intercept.

However, the estimation of errors in T_1 is troublesome. For instance, Mao [25] performed a study of 200 inversion-recovery experiments on ^{17}O relaxation in water. He found that the statistical error in T_1 is about six times as large as that reported by nonlinear least squares software. NLS software usually assumes linear approximation inference regions [26], and this assumption is often found to be inadequate. We advocate implementing an exact forward modeling approach to the problem of estimating mono-exponential decay in NMR.

The results of fitting the data to equation (16) are displayed in Figure 2. This is linear regression because the unknown parameters in equation (7) appear in that equation as linear parameters, although the calculated fitting functions are curved. There is great advantage to linear regression. For one, the statistical estimates of the parameters are well behaved. The coefficient of determination in this analysis is 0.9686.

This analysis leads to values for $(T_{1bound} + \tau_{bound})$ of 0.0054 ± 0.0008 s for CH_3 and 0.0074 ± 0.0011 s for CH_2. Since these values are significantly different (p < 0.1), it can be concluded that differences in T_{1bound} for ethanol CH_2 and CH_3 account for the difference and that τ_{bound} is small by comparison, otherwise the ratio of T_{1bound} for CH_2 and CH_3 would be unreasonable. If τ_{bound} is small then this is one more piece of supporting evidence that this chemical exchange occurs in the fast exchange limit. The values for ethanol CH_2 and CH_3 here are of similar magnitude to the value of $(T_{1bound} + \tau_{bound}) = (9.9 \pm 0.8) \times 10^{-3}$ s, for nicotine binding to asolectin solubilized nAChR found by authors in ref. [21], by monitoring relaxation of the proton *para* to the aromatic nitrogen. This similarity is supporting evidence for a likeness in stoichiometry of binding [18, 21].

Given that $\tau_{bound} \ll T_{1bound}$, then $\tau_{bound} < 0.0027 \pm 0.0004$ s, and $k_{-1} > 370 \pm 55 \, s^{-1}$.

The residuals displayed in Figure 2 provide insight into the nature of the error. It is seen that there is a consistency in absolute error in R_1. Consequently, the relative error in R_1 is inversely related to the magnitude of R_1 and proportional to T_1. As the magnitude of T_1 grows, its absolute error grows even faster. This is consistent with experience. Long T_1 times are difficult to measure accurately. Tables I and II show the calculation of the propagation of errors as percentage and absolute errors in T_1 for each concentration and thence to T_{1p} errors and weights. Figure 3 displays a T_{1p}

transformation of the data and curves of Figure 2, which suggests the use of extrapolation for the determination of K_d. Extrapolation of points at low concentration provides an estimate of $K_d = 122 \pm 258$ μM. (See discussion below.) The T_1 values and uncertainties estimated in Table 1 are used to calculate T_{1p} values and weights in Table 2. Also, shown in Table 2 are fitted values and residuals according to the model:

$$CH_2 T_{1p} \; = \; S_1 \{ [EtOH]_0 \, - \, K_d \} \qquad\qquad (19)$$

$$CH_3 T_{1p} \; = \; S_2 \{ [EtOH]_0 \, - \, K_d \} \qquad\qquad (20)$$

and shown as Navon analysis in Figure 3. In this linear analysis, the intercept has a large standard deviation 0.188 and a small positive value 0.0188. Accordingly, we set the best estimate, $0 < K_d < 0.17$ mM. From this analysis [27], we can set a 95% confidence range for K_d as [0, 0.46 mM].

Evaluation of Navon Analysis

Navon analysis [21, 22] is an approximation which provides approximate conclusions but which avoids otherwise very difficult analysis. The level of approximation involved in the Navon treatment may be justified when the level of approximation involved in the treatment of NMR relaxation is considered. However, since we propose an exact treatment of NMR relaxation, a second look at the Navon approximation is warranted.

The three equations that define equilibrium in a two-site chemical exchange can be solved [18]. To simplify notation, we use E to represent AChR. These equations are:

$$K_d = \frac{[L][E]}{[E \cdot L]}, \tag{21}$$

$$[L]_0 = [L] + [E \cdot L] \text{ and} \tag{22}$$

$$[R]_0 = [R] + [E \cdot L], \tag{23}$$

a system of three equations in three unknowns that is solved when:

$$[L] = [L]_0 - [E \cdot L], \tag{24}$$

$$[E] = [E]_0 - [E \cdot L], \text{ and} \tag{25}$$

$$[E \cdot L] = \text{RootOf}(Z^2 + (-K_d - [L]_0 - [E]_0)Z + [L]_0[E]_0). \tag{26}$$

We must choose the positive root of the polynomial for a physically reasonable solution. Hence,

$$[E \cdot L] = \frac{K_d + [E]_0 + [L]_0 + \sqrt{(K_d + [E]_0 + [L]_0)^2 - 4[L]_0[E]_0}}{2}. \tag{27}$$

$[L]_0$ is the independent variable, the initial ligand concentration. Using this exact formulation of equilibrium, we can simulate [18] the functional form of NMR relaxation with assumed parameter values. For example, Figure 4 plots the functional form of T_{1obs} for two-site exchange given some presumed values. Examination of the shape of

the curve at low ligand concentration shows that this curve is not exactly rectangular

hyperbolic, which is assumed for Navon linearization. Figure 5 shows the exact

functional form of T_{Ip} given some presumed parameter values. It is not exactly a

straight line, curvature at low concentrations is pronounced. In this simulation, a value

of K_d = 0.1 mM was assumed but extrapolation of the straight portion of the curve

back unto the negative x-axis predicts a value of K_d = 0.2 mM, according to the Navon

method. Hence, we can say that the Navon method is likely to underestimate binding

affinity by a factor of about two.

We had said that weighted Navon analysis predicts that $0 < K_d < 170$ µM for a

95% confidence interval of [0, 460 µM], for the binding of ethanol to nAChR. With this

new evaluation of the Navon method, we are better to say that analysis of the data

predicts that $0 < K_d < 85$ µM. This value is consistent with some estimates of the

affinity of ethanol for neuronal AChRs [28]. Extrapolation of points at low concentration

would suggest K_d is around 61 µM.   Additional analysis [18] in the context of rigorous

limits [27, 29] for nonlinear regression analysis that does not assume linear

approximation inference regions [26], provides a best estimate of K_d = 55 µM within a

90% confidence range of [0.5, 440 µM]. This similarity to the 95% confidence interval for

Navon analysis supports the use of the Navon approximation.

A Putative Site of Action

The ethanol molecule can be considered as a rigid electric dipole. When two isolated dipoles achieve a position of closet approach, energy minimization selects an orientation in which the two dipoles cancel, creating effectively, a nonpolar assembly. Sacco and Holtz [10, 11] used NMR measurement of intermolecular dipole-dipole relaxation rates and of self-diffusion coefficients of ethanol molecules to establish that ethanol self-association occurs in aqueous media, but only at molar concentrations. An ethanol dimer retains an electric quadrupole moment that is effective over short range. Cohen et al. [30] used [^{3}H]acetylcholine mustard to identify residues contributing to the cation-binding subsite of the nicotinic acetylcholine receptor. A representative sequence alignment of the cation-binding subsite is shown below:

```
LPSDDVWLPDLVLYNNADGDFAIVHMTK Torpedo californica (Pacific electric ray)

VPSEMIWIPDIVLYNNADGEFAVTHMTK alpha polypeptide 2 (human neuronal)

IPSELIWRPDIVLYNNADGDFAVTHLTK alpha polypeptide 4 (human neuronal)

IPSEKIWRPDLVLYNNADGDFAIVKFTK alpha polypeptide 1 (human neuromuscular)
```

BLAST search [31] of the nonredundant protein database at GenBank [32] reveals that the sequence PDIVLYNNADG, centered about tryrosine-93 (human neuromuscular numbering), is conserved in fish, mammal, bird, insect and amphibian. The importance of the cation-binding domain is further illustrated in the human neuromuscular junction

where it is found to be adjacent to the Main Immunogenic Region (MIR), α67-76 of the autoimmune disease Myasthenia Gravis [33].

We studied [18] the interaction of ethanol and the 28-residue cation-binding subsite, α80-107, of human neuromuscular nAChR. Secondary structure prediction algorithms [34-40] assign very weak structure forming elements to this sequence [34-40]. This prediction is consistent with observations made using heteronuclear and multidimensional NMR methods [18]. There is little consensus among the various secondary structure prediction algorithms, except for a prediction of beta-sheet near the central tyrosine. Examination of the Kyte-Doolittle hydropathy plot [41] for this sequence shows a relatively flat hydropathy in the middle of the peptide, with a more hydrophilic N-terminal end and more hydrophobic C-terminal end. If a 28 residue peptide sequence is truly a random coil, it is predicted to sample nearly 9^{27} = 4.39E695 backbone conformations. Given the shape of the hydropathy plot, we predict this peptide to be condensed in aqueous solution and to sample a smaller conformation space.

The formation of nonpolar molecular assemblies is disfavored in a polar medium but favored in a nonpolar environment. Energy minimization predicts that if an ethanol dimer is found within the nonpolar environment of a protein near an ionizable phenolic tyrosine hydroxyl, that the proton and two ethanol molecules should form a charged nonpolar molecular assembly. Furthermore, such an assembly is predicted to have

about the same volume and charge distribution as the choline head group. We observed [18] dramatic change in the proton spectrum of 28mer, most notably in the amide region, induced in the peptide by choline, indication of a change in the ensemble of sampled conformations.

NMR relaxation studies [18] of the interaction of ethanol and cation-binding subsite peptide of human neuromuscular nAChR established that ethanol binds with a stoichiometry of two. Downfield chemical shifts of methylene protons, like a model system [18], indicate that bound ethanol interacts with a proton. From nonlinear regression analysis, the best estimate of one binding constant (that of least affinity) is K_d = 39 ± 13 μM at 4 °C. This estimate is within the uncertainty range of the best estimate of the binding affinity of ethanol for the nicotinic acetylcholine receptor, K_d = 55 μM. This establishes that the cationic-binding subsite is a putative site of action of ethanol and that tyrosine-93 is implicated in the binding.

Discussion

In this study, we have used nuclear magnetic resonance techniques to examine the interaction of ethanol with the acetylcholine receptor. Studies on the effects of ethanol on ligand-gated ion channels such as the acetylcholine receptor have used various functional measurements to study the interaction of ethanol with the receptor [51]. While these types of studies have provided great insight into the mechanism of

ethanol's effects on the channel, and even the site(s) of action, they do not directly study the binding reaction between ethanol and the receptor. NMR relaxation methods offer one means of directly measuring the affinity of ethanol for the receptor.

The first biological NMR binding constant determination used chemical shift measurements to study the association equilibria of N-acetyl-D-glucosamine anomers and lysozyme [42]. Later, the determination of binding constants by line width measurements was applied to sulphanilamide binding to bovine carbonic anhydrase [43]. This work was followed by the determination of τ_c for various inhibitors bound to carbonic anhydrase, using T_1 and T_2 measurements at three magnetic field strengths [44]. Biological NMR binding constant determination in the context of nicotinic pharmacology, was first applied to the binding of nicotine to asolectin solubilized nAChR protein using the selective T_{1p} method [21]. This work was followed by binding constant measurement for various ligands to recombinant active site peptides of the nicotinic acetylcholine receptor using the selective T_{1p} method [22]. NMR binding constant estimates agree with estimates obtained by other methods (when available) to within experimental error. A recent validation of this statement, compared NMR binding measurements to kinetics binding measurements, for Vanadium(V) binding to ribonuclease A [45]. This work was later confirmed by other authors [46].

In this study, we obtained an estimate for the dissociation constant for ethanol from cholate-solubilized nicotinic acetylcholine receptors on the order of 50-100 μM.

This value is like the concentrations of ethanol that altered the gating of AChRs in PC12 cells [28]. However, this is much lower than blood alcohol levels associated with intoxication (on the order of 20 mM), as well as the concentrations of ethanol that enhance *Torpedo* nAChR gating   [47].

The discrepancy between the estimate of the dissociation constant for ethanol binding to the Torpedo receptor and functional measurements on the same receptor could be due to several possibilities. First, the receptor in the NMR experiments may be in the denatured state, and thus ethanol is binding to a completely different conformation of the receptor than studies in the functional state. We consider this unlikely because of the line-broadening of ethanol, which disappears with time as the protein denatures. Since this line broadening is observed in the time scale of our experiments, we assume that the protein is still in a native-like conformation. Second, and more likely, is that like all direct measurements of binding, the site with the highest affinity is the easiest to detect, and in the case of the Torpedo AChR, the highest-affinity site is not necessarily the one responsible for most of the functional consequences of the interaction of ethanol with the receptor. If this is true, then while we have determined the affinity of a site for the interaction of ethanol with the AChR, it may not be the one associated with the alterations in nAChR gating.

Even if the site we have studied is not the one responsible for functional alterations associated with ethanol's actions, we have demonstrated that it is possible to use NMR analysis to examine the interaction of small-molecules with ligand-gated ion channels. Extension of this technique to any one of several channel modulators with

affinities in the micromolar range (which are generally too low to measure with conventional ligand-binding techniques) should allow one to begin to understand the nature of the interaction of these modulators with the channels, and potentially help determine the site(s) of action of these compounds.

Acknowledgments

References

1. K.K. Grant. (1994) Behav Pharmacol 5, 383-404
2. D.M. Lovinger, G. White and F.F. Weight. (1989) Science 243, 1721-4
3. G. Wu, P.H. Tonner and K.W. Miller. (1994) Mol Pharmacol 45, 102-8
4. C. Li, R.W. Peoples and F.F. Weight. (1994) Proc Natl Acad Sci U S A 91, 8200-4
5. N.P. Franks and W.R. Lieb. (1994) Nature 367, 607-14
6. T. Yamakura, S.J. Mihic and R.A. Harris. (1999) J Biol Chem 274, 23006-12
7. Q.L. Zhou, Q. Zhou and S.A. Forman. (2000) Biochemistry 39, 14920-6
8. V.A. Daragan, A.M. Voloshin, S.V. Chochina, T.N. Khazanovich, W.G. Wood, N.A. Avdulov and K.H. Mayo. (2000) Biophys J 79, 406-15
9. J.M. Moore. (1999) Biopolymers 51, 221-43
10. A. Sacco and M. Holz. (1997) J. Chem. Soc., Faraday Trans. 93, 1101-1104
11. A. Sacco, F.M. De Cillis and M. Holz. (1998) J. Chem. Soc., Faraday Trans. 94, 2089-2092
12. D.E. Wemmer and P.G. Williams. (1994) Methods Enzymol 239, 739-67
13. R.L. Huganir and E. Racker. (1982) J Biol Chem 257, 9372-8
14. A. Sobel, M. Weber and J.P. Changeux. (1977) Eur J Biochem 80, 215-24

15. M. Epstein and E. Racker. (1978) J Biol Chem 253, 6660-2

16. J.C. Meunier, R. Sealock, R. Olsen and J.P. Changeux. (1974) Eur J Biochem 45, 371-94

17. H. Katki, G.H. Weiss, J.E. Kiefer, H. Taitelbaum and R.G. Spencer. (1996) NMR Biomed 9, 135-9

18. D.G. Naugler. (2001). Spectral Estimation of NMR Relaxation: A Consequence of a Study of Ethanol Neurotoxicity, Ph.D. thesis. Simon Fraser Univ. 218 pp.

19. A. Cornish-Bowden. (1995) Analysis of Enzyme Kinetic Data, Oxford University Press

20. D.G. Naugler and R.J. Cushley. (2000) J. Magn. Reson. 145, 209–215

21. R.W. Behling, T. Yamane, G. Navon, M.J. Sammon and L.W. Jelinski. (1988) Biophys J 53, 947-54

22. Y. Fraenkel, B. Ohana, J.M. Gershoni and G. Navon. (1991) J Basic Clin Physiol Pharmacol 2, 207-15

23. H.M. McConnell. (1958) J. Chem. Phys. 28, 430-431

24. R.W. Behling, T. Yamane, G. Navon and L.W. Jelinski. (1988) Proc Natl Acad Sci U S A 85, 6721-5

25. X. Mao. (1993) Appl. Magn. Reson. 4, 261-264

26. D.M. Bates and D.G. Watts. (1988) Nonlinear regression analysis and its applications, John Wiley & Sons, New York

27. MicroMath. (1995), 2.01 ed., MicroMath Scientific Software Inc., Salt Lake City, UT

28. K. Nagata, G.L. Aistrup, C.S. Huang, W. Marszalec, J.H. Song, J.Z. Yeh and T. Narahashi. (1996) Neurosci Lett 217, 189-93

29. G.E.P. Box, W.G. Hunter and J.S. Hunter. (1978) Statistics for Experimenters, An Introduction to Design, Data Analysis, and Model Building, John Wiley & Sons

30. J.B. Cohen, S.D. Sharp and W.S. Liu. (1991) J Biol Chem 266, 23354-64

31. S.F. Altschul, T.L. Madden, A.A. Schaffer, J. Zhang, Z. Zhang, W. Miller and D.J. Lipman. (1997) Nucleic Acids Res 25, 3389-402

32. C. Burks, J.W. Fickett, W.B. Goad, M. Kanehisa, F.I. Lewitter, W.P. Rindone, C.D. Swindell, C.S. Tung and H.S. Bilofsky. (1985) Comput Appl Biosci 1, 225-33

33. P. Orlewski, M. Marraud, M.T. Cung, V. Tsikaris, M. Sakarellos-Daitsiotis, C. Sakarellos, E. Vatzaki and S.J. Tzartos. (1996) Biopolymers 40, 419-32

34. P.Y. Chou and G.D. Fasman. (1974) Biochemistry 13, 222-45

35. A.A. Salamov and V.V. Solovyev. (1995) J Mol Biol 247, 11-5

36. A.A. Salamov and V.V. Solovyev. (1997) J Mol Biol 268, 31-6

37. V.V. Solovyev and A.A. Salamov. (1991) Molek. Biol. 25, 810-824

38. V.V. Solovyev and A.A. Salamov. (1994) Comput Appl Biosci 10, 661-9

39. V.V. Solovyev and A.A. Salamov. (1994) in Computer analysis of Genetic macromolecules (N.A. Kolchanov and H.A. Lim, eds.), pp. 352-364, World Scientific

40. J. Garnier, D.J. Osguthorpe and B. Robson. (1978) J Mol Biol 120, 97-120

41. J. Kyte and R.F. Doolittle. (1982) J Mol Biol 157, 105-3

42. F.W. Dahlquist and M.A. Raftery. (1968) Biochemistry 7, 3269-76

43. A. Lanir and G. Navon. (1971) Biochemistry 10, 1024-32

44. G. Navon and A. Lanir. (1972) J. Magn. Reson. 8, 144-151
45. C.H. Leon-Lai, M.J. Gresser and A.S. Tracey. (1996) Can. J. Chem. 74, 38-48
46. J.M. Messmore and R.T. Raines. (2000) Journal of the American Chemical Society 122, 9911 – 9916
47. S.A. Forman, D.L. Righi and K.W. Miller. (1989) Biochim Biophys Acta 987, 95-103
48. Naugler, David (2017), "FORTRAN code addendum for JMR 145, 209–215 (2000)", Mendeley Data, v1 http://dx.doi.org/10.17632/5f4ypf6j4v.1
49. Naugler, David (2017), "INTERIM REPORT I.", Mendeley Data, v1 http://dx.doi.org/10.17632/45k7w82byr.1
50. Naugler, David (2017), "INTERIM REPORT II.", Mendeley Data, v1 http://dx.doi.org/10.17632/42n45mkstx.1
51. Davis, T. J., & de Fiebre, C. M. (2006). Alcohol's actions on neuronal nicotinic acetylcholine receptors. Alcohol Research and Health, 29(3), 179
52. Naugler, D. G., & Cushley, R. J. (1983). Nonlinear regression models of multicomponent interactions of anhydropolyols with aqueous ammonium ion by carbon-13 nuclear magnetic resonance. *The Journal of Physical Chemistry*, *87*(23), 4720-4724.

Table 1

T_1 and T_{1p} Values and Uncertainties

[EtOH]	CH$_2$ T$_1$	CH$_3$ T$_1$	% error	CH$_2$ T$_1$ error	CH$_3$ T$_1$ error	CH$_2$ T$_{1p}$	CH$_2$ T$_{1p}$ error	CH$_3$ T$_{1p}$	CH$_3$ T$_{1p}$ error
1.34	2.949	2.394	5%	0.15	0.12	6.34	1.0	4.49	0.57
2.67	3.904	3.121	7%	0.27	0.22	13.34	4.51	7.96	1.88
3.89	4.577	3.942	8%	0.37	0.32	26.86	18.23	16.98	8.15
7.23	5.059	4.254	9%	0.46	0.38	60.94	94.65	24.82	17.59
free	5.517	5.134	10%	0.55	0.51				

Table 2

T_{1p} Values, Weights and Fit

[EtOH]	CH$_2$ T$_{1p}$	CH$_2$ weight	CH$_3$ T$_{1p}$	CH$_3$ weight	CH$_2$ T$_{1p}$ calculated	CH$_3$ T$_{1p}$ calculated	CH$_2$ T$_{1p}$ residuals	CH$_3$ T$_{1p}$ residuals
1.34	6.34	1	4.49	3.077	6.462	4.395	-0.122	0.0949
2.67	13.34	0.049	7.96	0.28	12.967	8.819	0.372	-0.859
3.89	26.86	0.0030	16.98	0.015	18.934	12.877	7.925	4.102
7.23	60.94	0.00011	24.82	0.0032	35.271	23.988	25.668	0.831

Figure Legends

Figure 1.   The bottom trace, A, shows the spectrum of 1% sodium cholate in D_2O with ethanol at approximately 7 mM. In the spectrum of the top trace, B, nAChR protein (1.7 µM, not visible) is solubilized with 1% sodium cholate in D_2O and ethanol is present at approximately 7 mM. The resonance at 1.0 ppm is the methyl and that at 3.5 ppm is the methylene of ethanol.

Figure 2. Plot of reduced relaxation rate of ethanol CH_3 and CH_2 protons versus ethanol concentration. A least square 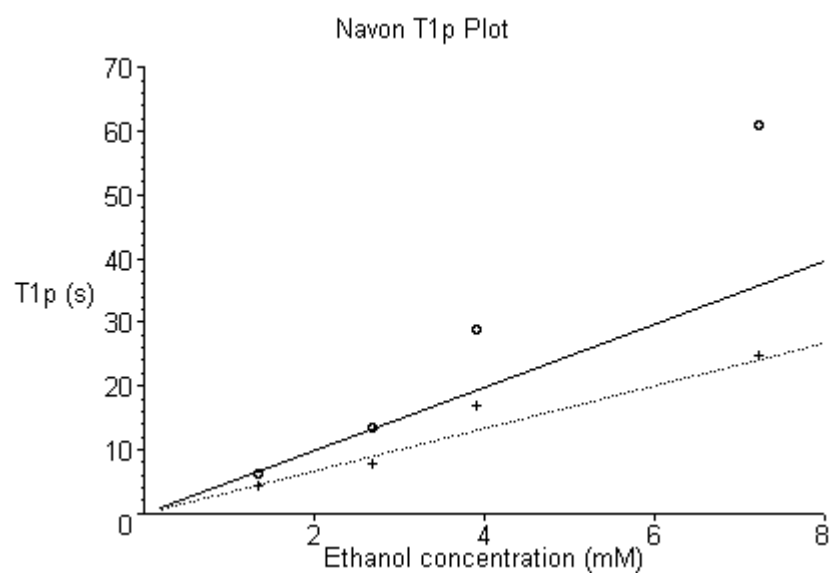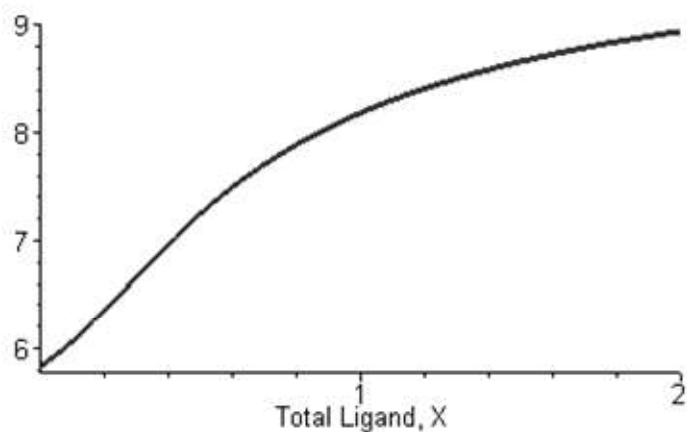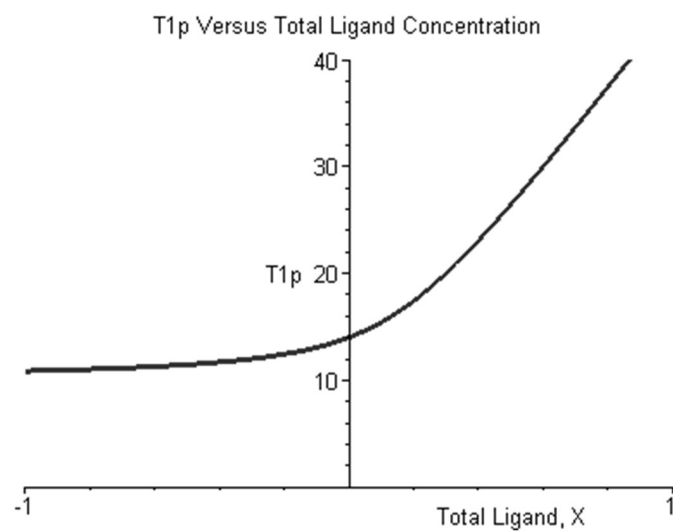fit of the tight binding model, $K_d=0$ reproduces the relaxation data with coefficient of determination 0.976 The model reproduces relaxation data for 'free' ethanol exactly. The solid line and circles relate to CH_2 protons, dotted line and crosses relate to CH_3 protons.

Figure 3. Navon T_{1p} plot of CH_3 and CH_2 proton relaxation data versus ethanol concentration shows how the data and least squares curves of Figure 2 transform under the T_{1p} formulation. The solid line and circles relate to CH_2 protons, dotted line and crosses relate to CH_3 protons. The T_{1p} value of 'free' ethanol is infinite because of numerical instability. Extrapolation of points at low concentration provides an estimate of $K_d = 122 \pm 258$ µM.

Figure 4. Plot of predicted T_1 versus ethanol concentration, assuming $K_d = 0.1$ mM, showing the calculated variation of T_1 with variation of total ligand concentration, $X = [L]_0$.

Figure 5. Plot of the calculated variation of T_{1p} with variation of total ligand concentration and setting $K_d = 0.1$ mM. For purposes of demonstration, the plot is extended into the region of physically unrealizable negative ligand concentration. On the right, the curve is asymptotically linear extrapolation from the linear region onto the negative x-axis gives an intercept of -0.2 mM.
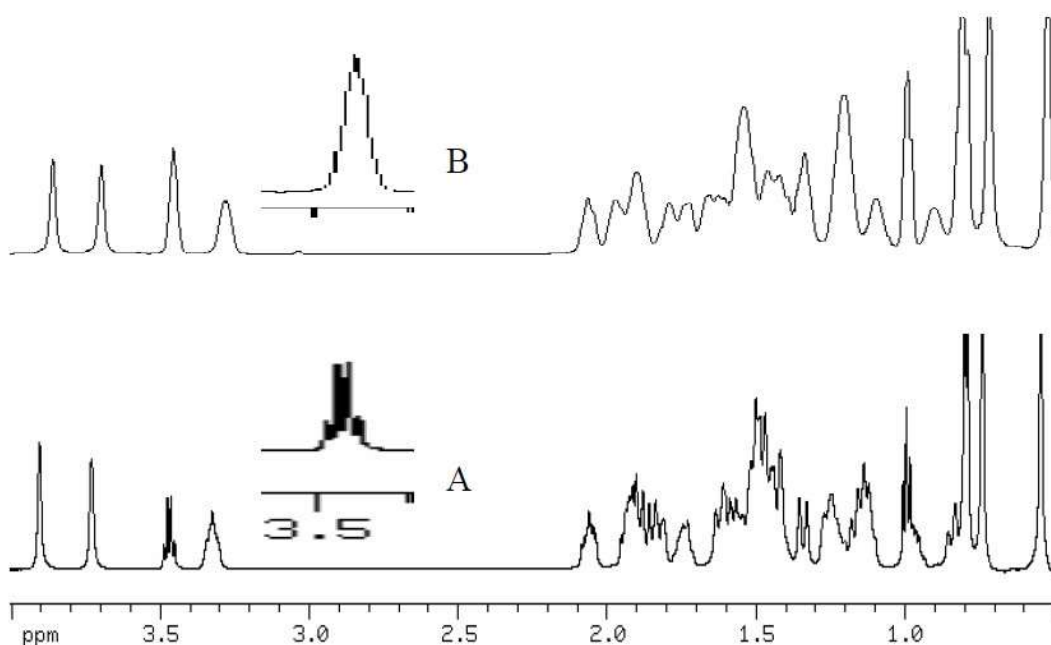

Figure 1

1.7 microMolar nAChR

Figure 2

Navon T1p Plot

Figure 3

Figure 4

Figure 5

Figure Legends

Figure 1.   The bottom trace, A, shows the spectrum of 1% sodium cholate in D_2O with ethanol at approximately 7 mM. In the spectrum of the top trace, B, nAChR protein (1.7 µM, not visible) is solubilized with 1% sodium cholate in D_2O and ethanol is present at approximately 7 mM. The resonance at 1.0 ppm is the methyl and that at 3.5 ppm is the methylene of ethanol.

Figure 2. Plot of reduced relaxation rate of ethanol CH_3 and CH_2 protons versus ethanol concentration. A least square fit of the tight binding model, K_d=0 reproduces the relaxation data with coefficient of determination 0.976 The model reproduces relaxation data for 'free' ethanol exactly. The solid line and circles relate to CH_2 protons, dotted line and crosses relate to CH_3 protons.

Figure 3. Navon T_{1p} plot of CH_3 and CH_2 proton relaxation data versus ethanol concentration shows how the data and least squares curves of Figure 2 transform under the T_{1p} formulation. The solid line and circles relate to CH_2 protons, dotted line and crosses relate to CH_3 protons. The T_{1p} value of 'free' ethanol is infinite because of numerical instability. Extrapolation of points at low concentration provides an estimate of $K_d = 122 \pm 258$ µM.

Figure 4. Plot of predicted T_1 versus ethanol concentration, assuming $K_d = 0.1$ mM, showing the calculated variation of T_1 with variation of total ligand concentration, $X = [L]_0$.

Figure 5. Plot of the calculated variation of T_{1p} with variation of total ligand concentration and setting $K_d = 0.1$ mM. For purposes of demonstration, the plot is extended into the region of physically unrealizable negative ligand concentration. On the right, the curve is asymptotically linear extrapolation from the linear region onto the negative x-axis gives an intercept of -0.2 mM.
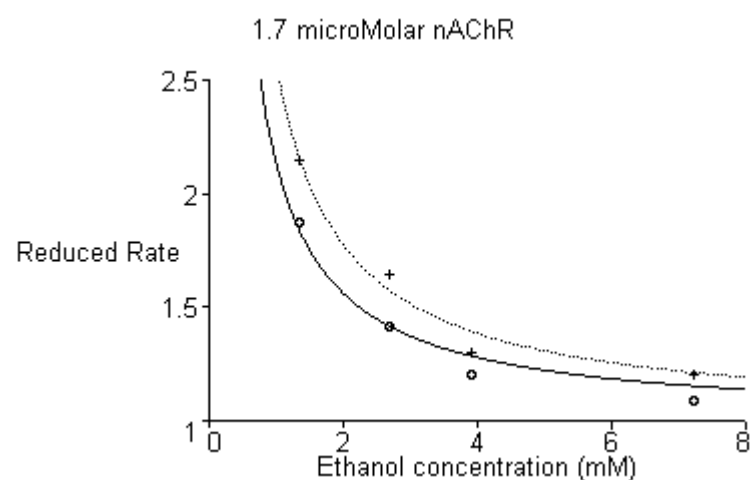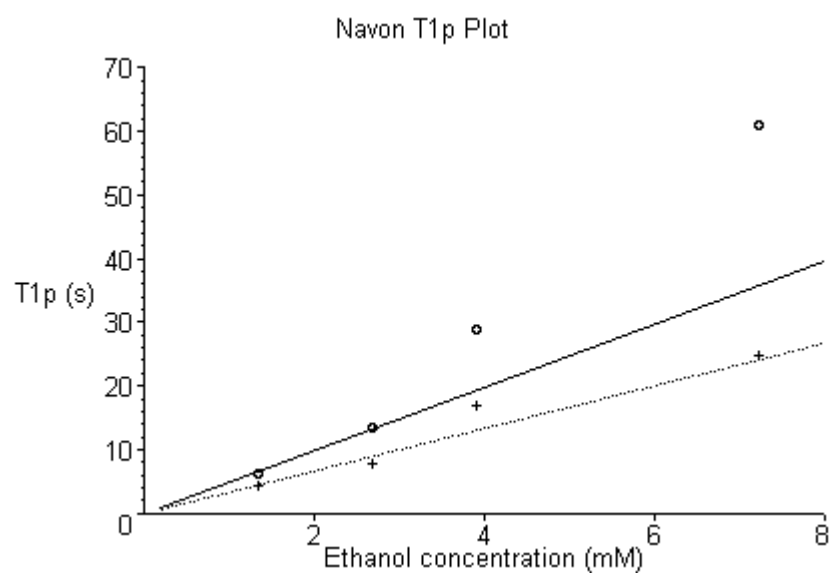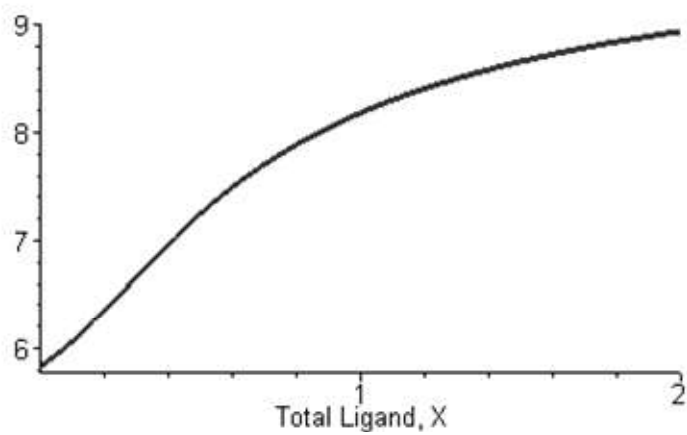

Figure 1

1.7 microMolar nAChR

Figure 2

Navon T1ρ Plot

Figure 3

Figure 4

Figure 5